

## Experimental Testing of Basic Crash Elements Made of CFRP by Additive Technologies

Tomáš Kalina, Stanislav Špírk, František Sedláček

Faculty of Mechanical Engineering, University of West Bohemia, 306 14 Pilsen. Czech Republic. E-mail: [tkalina@fst.zcu.cz](mailto:tkalina@fst.zcu.cz), [spirks@fst.zcu.cz](mailto:spirks@fst.zcu.cz), [fsedlace@fst.zcu.cz](mailto:fsedlace@fst.zcu.cz)

This paper deals with the experimental testing of the basic crash elements which are made of PA6 with short carbon fiber reinforcement by additive technology. Additive technologies allow the production of very complex, thin-walled and hollow shapes, which can be used to tune the desired characteristics of the deformation member. The variable size of the deceleration, the length of the deformed part and the total amount of energy absorbed can be controlled by suitable geometry. The initial impact peaks can be reduced by gradually changing the geometry. Experimental testing of the basic crash elements was performed on several specimens and average values are used in this paper. The maximal and the average deceleration and total energy absorbed are primarily monitored. The obtained data will be used for validation of material properties in Crash-Pam software. Usage of a validated material model, larger and more complex deformation members will be proposed, e.g. for the racing car Formula SAE.

**Keywords:** Crash element, Impact attenuator, Additive technologies, CFRP, Formula SAE

### 1 Introduction

All road vehicles, whether normal traffic or racing cars, place great emphasis on the **safety of the crew** [1]. One of the basic elements of vehicle passive safety is the **Energy absorption element** that is also called the **Impact attenuator** in **Formula SAE**. The basic frontal Impact attenuator is also designed and manufactured in Formula SAE (FSAE). Currently, most of ten FSAE uses impact attenuator made of hardened or metal foams, aramid or aluminium alloy honeycombs. These types of impact attenuators are used for their very good weight-to-energy ratio as well as for keeping the limits for average and maximum vehicle deceleration at the defined impact.

However, due to production technology (mainly **honeycombs** [2]) the possibilities of the impact attenuator shape is limited. We are able to produce complex shapes using additive technologies. Therefore, we could afford to **optimize** the shape of the impact attenuator for better deceleration characteristics and very low weight.

The energy absorption elements made by additive technologies **are not commonly used in road vehicles yet**. But there is a research that examines a **metal crash-boxes with a printed filling** from nylon [3].

The deformation elements are created by means of various metal **crash-box elements** [4], [5] and **bumpers** [5] made of shaped steel sheets in conventional road vehicles. Alternatively, they can be supplemented with various plastic or hardened or metal foams components [5]. However, conventional road vehicles are significantly heavier than the aforementioned FSAE

vehicles and are also designed for collisions at higher speeds. Their deformation zones are therefore dimensioned for significantly greater energy absorption. The deformation elements made of **composite parts** [6] are used only in luxury or sports cars. Their main advantage is low weight, but their big disadvantage is a high price.

### 2 Standard impact attenuators in Formula SAE

The Impact attenuators are made in FSAE from various perforated **sheets** of steel or aluminum alloys [4], [5], hardened or metal **foams** [5], aluminum or composite **honeycombs** [2], etc. [7] The usage of each of these materials has its advantages and disadvantages. The sheet metal impact attenuators are generally heavier than those made of foam or honeycombs, which are generally standard today. Also the deformation members are made of **composite laminates**, which are very expensive and difficult to manufacture. The honeycombs, the foams and the laminates are usually glued [8] to impact the attenuator plate [9].

For example, the impact attenuators that have been tested for UWB vehicles (University of West Bohemia) and meet FSAE requirements that are: The aluminum alloy honeycomb impact attenuator of 200x200x100 mm weights 365 g and the aramid honeycomb impact attenuator of 200x200x100 mm with a relief holes weights 332 g.

The rules [9] consider that IA assembly (impact attenuator (crash element), impact attenuator plate and

fasteners) is mounted on the front of a vehicle with a total mass of 300 kg and impacting a solid, non-yielding impact barrier with a velocity of impact of 7 m/s. Impact attenuators appropriate to FSAE rules shall absorb a minimum deformation energy of 7350 J with a maximum deceleration not exceeding 40 g and an average deceleration not exceeding 20 g. The minimum dimensions of the impact attenuators for FSAE are 200x200x100 mm but may not be fully filled. Holes can be formed in it [9].

### 3 Basic crash elements - characteristics

The aim of this article is to determine the basic mechanical properties of the material during the crash. PA6 with short carbon fiber reinforcement (PA6+SCF/CFRP) using the **additive technology** was chosen as the tested material. The geometry of the basic crash elements was also designed for testing, which is adapted to the available test equipment as well as the technological capabilities of the printer (**3D printer Mark Two made by Markforged**).

Basic dimensions of basic crash elements are 90x90x90 mm. Basic crash elements are designed as 'Truncated cones' shells with anchoring base. The print settings are described in Tab. 1 and geometric properties of basic crash elements are specified by Tab. 2 and Fig. 1.

Tab. 1 Setting of the 3D printer Mark Two (Markforged)

Width injection [mm]	0.4
Height Layers [mm]	0.1
Fill Pattern [-]	Triangular
Fill Density [%]	28
Roof Layers [-]	1
Floor Layers [-]	1
Wall Layers [-]	1

Tab. 2 Properties of the basic crash elements

Number Layers [-]	900
Height [mm]	90
Mass [g]	35.2
Volume [mm <sup>3</sup> ]	72 793
Printing time [h]	10.4
Material	ONYX (PA6+SCF) [10]

The paper [11], which was created in our department, deals with the determination of basic material parameters of PA6+SCF [11], [12]. This material is manufactured by Markforged company for the Mark Two printers with the trade name ONYX [10].

**HPS (Horizontally Printed Specimens) from PA6 and PA6+SCF.** These specimens were printed horizontally on the building platform. The angle between the main direction of the filaments and the testing direction was 0°. Average measured data for individual temperatures are given in Fig. 2 [11].

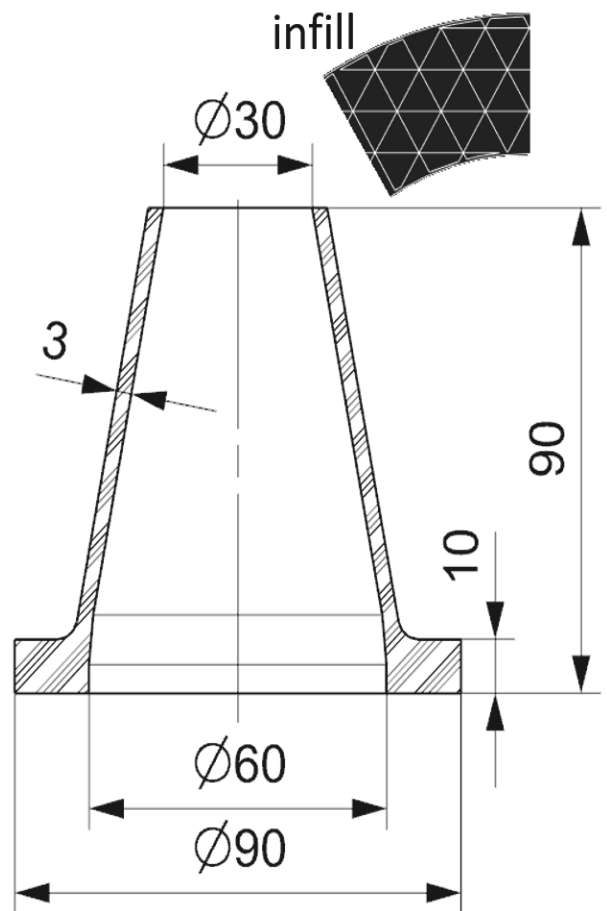


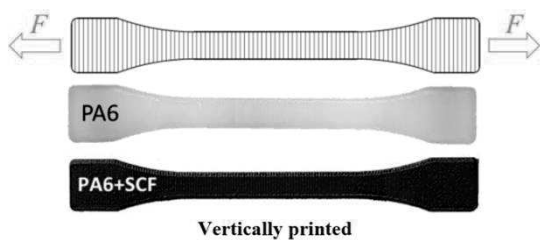
Fig. 1 Geometry of basic crash elements



T [°C]	Horizontally printed		
	$E_t$ [MPa] PA6+SCF/PA6	$\sigma_M$ [MPa] PA6+SCF/PA6	$\epsilon_M$ [%] PA6+SCF/PA6
20	1093/456	47.3/41.1	182/194
40	921/389	41.4/37.5	216/217
60	715/264	38.3/28.4	224/249
80	690/170	36.5/19.2	231/293
100	604/-	33.8/-	228/-
120	559/-	30.7/-	244/-
140	477/-	27.4/-	249/-
160	342/-	23.6/-	258/-

Fig. 2 Average experimental data of HPS from PA6+CF [11]

**VPS (Vertically Printed Specimens) from PA6 and PA6+SCF.** These specimens were printed vertically on the building platform. The angle between the main direction of the filament and the testing direction was 90°. The average measured data for individual temperatures are given in Fig. 3 [11].



T [°C]	$E_r$ [MPa]	$\sigma_M$ [MPa]	$\epsilon_M$ [%]
	PA6+SCF/PA6	PA6+SCF/PA6	PA6+SCF/PA6
20	609/504	28.9/27.1	18.4/58.1
40	533/347	25.1/13.2	19.5/61.4
60	405/272	21.6/11.9	21.1/68.9
80	341/215	19.1/10.2	23.2/74.1
100	31/ -	16.3/ -	23.6/ -
120	294/ -	14.9/ -	24.4/ -
140	243/ -	12.6/ -	24.6/ -
160	202/ -	10.1/ -	24.9/ -

Fig. 3 The average experimental data of VPS from PA6+CF [11]

### 4 Experimental testing

Tab. 3 The properties of experimental testing

Number of specimens [-]	4
Ram weight [kg]	43.4
Fall height [mm]	500
Sampling frequency of the accelerometer [Hz]	38 400
Sampling period of the accelerometer [ms]	0.02604167

Experimental testing was performed on the **Fall-weight impact testing machine**. The ram's weight used was 43.4 kg and was dropped from the height of 500 mm above the sample. Ram deceleration was measured by accelerometer. The sampling frequency of the accelerometer was 38,400 Hz, that sam-

pling period was 0.02604167 ms. The properties of experimental testing are summarized in Tab. 3.

### 5 The results of experimental tests

As already mentioned, 4 experimental tests of the same specimens were made. The average values were determined from the tests and are presented.

Fig. 4 shows test specimens from slow-motion camera during experiment a) before impact, b) impacted specimen No. 2 and c) impacted specimen No. 4. Samples b) and c) are shown in the state between the 1st and the 2nd impact. All measured data are displayed for the 1st impact only. Secondary and other impacts caused by reflection by elastic deformation were cut off.

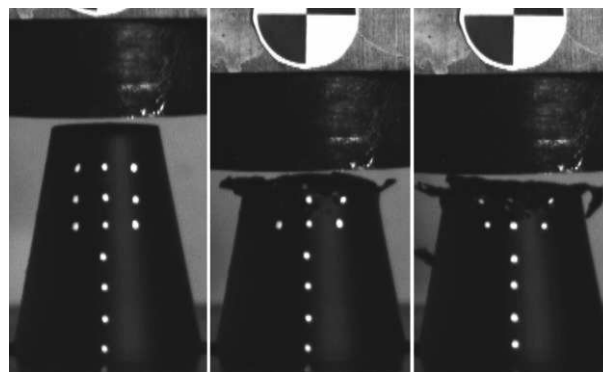


Fig. 4 Test specimens - a) before impact, b) and c) impacted specimens no. 2 and no. 4

Fig. 5 shows averaged measured values of 4 tests, simplified process and a linearized process of the middle section of deceleration-time diagram. In Tab. 4 shows the coordinates of simplified process curve. Individual points are connected by straight lines.

Tab. 5 summarizes the data determined from measurements and accelerometers.

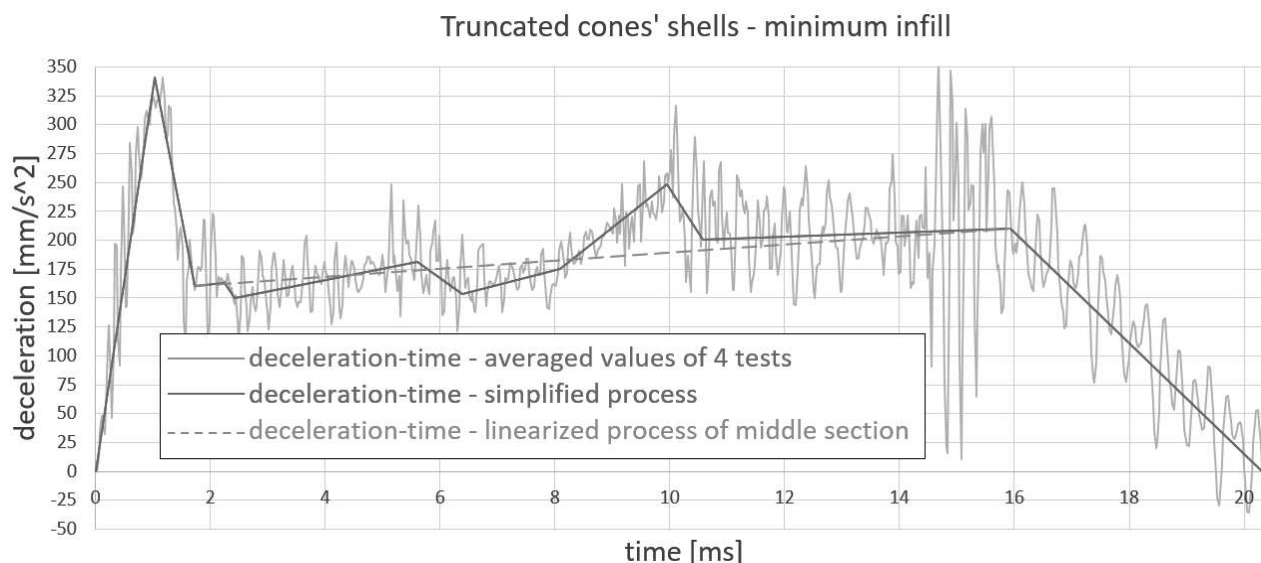


Fig. 5 Diagram deceleration-time

**Tab. 4** The coordinates of simplified deceleration-time process

point Nr.	time [ms]	deceleration [mm/s <sup>2</sup> ]
1	0.00	0.00
2	1.02	340.71
3	1.73	160.34
4	2.25	163.27
5	2.41	149.58
6	5.61	181.36
7	6.38	153.00
8	8.09	175.00
9	9.94	248.81
10	10.57	200.42
11	15.92	209.71
12	20.32	0.00

$$E_K = 0.5 \cdot m \cdot v^2 \rightarrow v = \sqrt{\frac{E}{0.5 \cdot m}} = \sqrt{\frac{212}{0.5 \cdot 43.3}} = 3.129 \frac{m}{s} \quad (3)$$

Where:

$E_P$  ... Potential energy [J],

$E_K$  ... Kinetic energy [J],

$m$  ... Mass [kg],

$g$  ... Gravitational acceleration [m/s<sup>2</sup>],

$h$  ... Height [m],

$v$  ... Velocity [m/s].

$$m_{PA-FSAE} = \frac{E_{PA-FSAE}}{E_{PA-S}} \cdot m_{PA-S} = \frac{7350}{212} \cdot 3.413 = 118 \text{ g} \quad (4)$$

Where:

$m_{PA-FSAE}$  ... Mass of the PA6+SCF deformation member complying with FSAE rules [g],

$m_{PA-S}$  ... Mass of the PA6+SCF deformed part of specimen [g],

$E_{PA-FSAE}$  ... Minimum required energy according to the FSAE rules [J],

$E_{PA-S}$  ... Deformation energy absorbed by deformed part of specimen (Fig. 6 - orange part) [J].



**Fig. 6** Specimen with highlighted (orange) deformed part of specimen

**Tab. 5** The parameters determined from the experiment

Deformed height [mm]	21
Total deformation time [ms]	20.3
Average deceleration [mm/s <sup>2</sup> ]	174.9
Maximum deceleration [mm/s <sup>2</sup> ]	340.8

## 6 The determination of deformation energy and velocity

The equation (1) describes the potential energy of the weight that falls from the rest position at a height of 500 mm above the specimen. The same amount of energy must be absorbed by the specimen. Here applies (2), the kinetic energy of the impact is equal to the potential energy of the lifted weight above the specimen. The equation (3) describes as determined by the velocity of the weights before impact from kinetic energy.

$$E_P = m \cdot g \cdot h = 43.3 \cdot 9.81 \cdot 0.5 = 212 \text{ J} \quad (1)$$

$$E_P = E_K \text{ [J]} \quad (2)$$

The equation (4) describes the determination of the real FSAE impact attenuator, assuming a linear dependence of energy and weight and absorption of the required deformation energy of 7350 J [9]. It is not assumed that by increasing the deformation member of PA6 + SCF, energy and weight will increase linearly. It is only a rough calculation, whether it makes sense to solve the deformation member from PA6 + SCF.

## 7 The discussion of results

The height of the 21 mm specimen was deformed during the experiment. The deformed volume corresponds to approximately 3.413 g of material, while absorbing energy of 212 J. Energy absorption of 7350 J is required according to FSAE requirements. The lowest weight of the proposed aramid honeycomb impact attenuator UWB is 332 g. If we consider linear increase of energy with increasing volume, specifically weight, so with a larger impact attenuator or a plurality of basic crash elements, we would achieve a weight of approximately 118 g to absorb energy 7350 J.

The diagram in Figure 5 can be divided into **three basic parts**. In the first part, which lasts less than 2ms, is **the initial peak**. During impact tests there is always an initial peak. The initial peak is caused by the initial resistance of the material on impact. A very high peak in connection with a deformation member can have negative effects on the crew, so there is an effort to reduce it. It is possible to adjust the size of the initial peak and its duration by using the appropriate geometry.

In the **second part**, the speed of the **ram gradually slows down** over a relatively long distance. This

section lasts approximately 14ms. The slow deceleration on a longer distance is suitable for the safety of the car's crew. In this part, the majority of the kinetic energy of the ram is also absorbed. This part of the diagram is not linear as we can observe jumps within it. These jumps can be caused by averaging several partial results but they are also caused by uneven filling in the thin-walled cones. If we intersect a straight line through this whole section we get a slightly increasing line. This is due to the fact that the specimen is conical in shape and during the deformation there is a gradual increase in the cross-sectional area. In the **third part**, the **ram stops** completely within 4ms.

## 8 Conclusion

The experimental tests of basic crash elements were performed, which will be used for material validation in Crash-Pam software.

It was estimated that the resulting weight of the deformation member made of PA6+SCF (ONYX) could reach to 118g, based on the measured results and using direct proportionality. It is more than twice less weight than that of the aramid deformation member.

Obviously, the increase will not be linear and other criteria, such as maximum and average deceleration, are also placed on the impact attenuators. However, this suggests some potential that there is a possibility to design a PA6 + SCF deformation member that will have the desired properties and will have a lower weight and possibly a better shape to hide at the tip of the car.

The additive technology gives us the possibility of a very complicated, hollow and thin-walled shapes, therefore a sophisticated impact attenuator will be developed based on these experiments, which could achieve better properties than the existing deformation members.

## Acknowledgement

*This paper is based on work sponsored by project SGS-2019-030 (Research and development of Advanced Components for the Formula Student Car - University of West Bohemia).*

## References

- [1] SPIRK, S. (2017) The collision of unbelted passenger with assessment of various vehicle interior. In: *Manufacturing Technology*, Vol.17, No.6, pp.962-969, UJEP, 2017, ISSN: 1213-2489.
- [2] SAENZ-DOMINGUEZ, I., TENA, I., ESNAOLA, A., SARRIONANDIA, M., TORRE, J., AURREKOETXEA, J. (2019). Design and characterisation of cellular composite structures for automotive crash-boxes manufactured by out of die ultraviolet cured pultrusion. In: *Composites Part B: Engineering*, Vol. 160, pp. 217-224, doi.org/10.1016/j.compositesb.2018.10.046
- [3] FU, X., ZHANG, X., HUANG, Z. (2020). Axial crushing of Nylon and Al/Nylon hybrid tubes by FDM 3D printing, In: *Composite Structures*, doi.org/10.1016/j.compstruct.2020.113055, IN PRESS, September 2020 Pre-proof
- [4] SHI, D., XIAO, X. (2018). An enhanced continuum damage mechanics model for crash simulation of composites. In: *Composite Structures*, Vol. 185, pp. 774-785, doi.org/10.1016/j.compstruct.2017.10.084
- [5] LI, Z., YU, Q., ZHAO, X., YU, M., SHI, P., YAND C. (2017) Crashworthiness and lightweight optimization to applied multiple materials and foam-filled front end structure of auto-body. In: *Advances in Mechanical Engineering*, Vol.9, No.8, pp.1-21, DOI: doi.org/10.1177/1687814017702806
- [6] HUSSAIN, N. N., REGALLA, S. P., DASESWARA RAO, Y. V. (2017). Low velocity Impact Characterization of Glass Fiber Reinforced Plastics for Application of Crash Box. In: *materialstoday*, Vol. 4, No. 2, Part A, pp.3252-3262, doi.org/10.1016/j.matpr.2017.02.211
- [7] RAZ, K., HORA, J., PAVLATA, P. (2017). Unconventional materials usage in design of vehicle bodies. In: *Manufacturing Technology*, Vol.17, No.5, pp.823-827, UJEP, 2017, ISSN: 1213-2489.
- [8] KALINA, T.; SEDLACEK, F. (2019). Design and Determination of Strength of Adhesive Bonded Joints. In: *Manufacturing Technology*, Vol.19, No.3, pp.409-413, UJEP, 2019, ISSN: 1213-2489, DOI: 10.21062/ujep/305.2019/a/1213-2489/mt/19/3/409
- [9] Formula student FSG RULES 2020. Online. 5.1.2020. www.fsg.one/rules
- [10] Material ONYX. Online. 5.1.2020. www.mar-kforged.com/materials/onyx/
- [11] SEDLACEK, F., LASOVA, V. (2018). Additive Manufacturing of PA6 with Short Carbon Fibre Reinforcement using Fused Deposition Modelling. *Materials Science Forum (MSF)*, Vol.928, pp.26-31, ICCMME 2018, Singapore, ISSN 0255-5476.
- [12] RAZ, K., ZAHALKA, M., CHVAL, Z., KUCEROVA, L. (2017). Analysis of Weld Line Influence on Strength of Nylon Parts. In: *Manufacturing Technology*, Vol.17, No.4, pp.561-565, UJEP, 2017, ISSN: 1213-2489